Microbes and Infection 27 (2025) 105466

Contents lists available at ScienceDirect

Microbes and Infection

journal homepage: www.elsevier.com/locate/micinf

HERV reactivation by adenovirus infection is associated with viral immune regulation

Wen Liang [a,b,1], Miona Stubbe [a,1], Lisa Pleninger [a,b], Anna Hofferek [a], Hans Stubbe [c,d], Julia Mai [f], Salih Özer [a,b], Dmitrij Frishman [e], Sabrina Schreiner [a,b,f,g,h,**], Michelle Vincendeau [a,b,*]

[a] Institute of Virology, School of Medicine, Technical University of Munich, Munich, Germany
[b] Institute of Virology, Helmholtz Zentrum München, Munich, Germany
[c] Medical Department II, University Hospital, LMU, Munich, Germany
[d] German Center for Infection Research (DZIF), Partner Site Munich, German, Germany
[e] Department of Bioinformatics, Technical University of Munich, 85354 Freising, Germany
[f] Institute of Virology, Medical Center - University of Freiburg, Freiburg, Germany
[g] Institute of Virology, Hannover Medical School, Hannover, Germany
[h] Cluster of Excellence RESIST (Resolving Infection Susceptibility; EXC 2155), Hannover Medical School, Hannover, Germany

ARTICLE INFO

Keywords:
HERVs
Differentially expressed HERVs
Differentially expressed genes
Human adenovirus
HAdV-C5
ERV-K9
FBXO17
Functional annotation
Gene regulation
INF response
Virus-host interactions

ABSTRACT

Human endogenous retroviruses (HERVs), which are normally silenced by methylation or mutation, can be reactivated by a variety of environmental factors, including infection with exogenous viruses. In this work, we investigated the transcriptional activity of HERVs following infection of human liver cells (HepaRG) with human adenovirus C serotype 5 (HAdV-C5). HAdV-C5 infection results in reactivation of several HERV groups as well as differentially expressed genes. Interestingly, in HAdV-C5 infection, upregulated genes that were in close chromosomal proximity to upregulated HERV loci were associated with influencing viral carcinogenesis and inflammatory signaling. We also identified an FBXO17 transcript encoding an intronic ERVK9-11 sense sequence upon HAdV-C5 infection. FBXO17 has previously been described as an important factor in the regulation of the interferon response. This suggests that specific HERV groups may have the potential to trigger gene networks and influence viral immune responses.

1. Introduction

A large proportion of the mammalian genome (46 %) is made up of mobile genetic elements called DNA transposons and retroelements, including human endogenous retroviral elements (HERVs) [1–5]. Approximately 8 % of the human genome consists of HERVs. In addition to complete, partially truncated and partially deleted HERV genomes, there are up to 500,000 copies of single long terminal repeats (LTRs) in the human genome [6]. Most HERVs have been silenced during evolution by mutation and/or epigenetic control. However, several HERV groups can be reactivated by environmental insults such as viral infections with exogenous viruses such as HIV-1 [7], HCV [8] or IAV [9]. Upon reactivation, HERVs can influence host gene expression through at least five mechanisms: (1) their LTRs can act as enhancer or repressor sites, (2) they can serve as promoter sites, (3) they provide polyadenylation signals to terminate transcripts, (4) they can provide splice sites, and (5) they can contribute to RNA interference [1,10,11]. HERV reactivation has also been shown to impact the immune response in various ways. For example, HERV-derived nucleic acids can activate pattern recognition receptors like RIG-I or toll-like receptors (TLRs) [12]. The HERV-W envelope protein has been reported to stimulate cytokine production via TLR signaling [13,14]. Additionally, HERV-derived proteins can trigger T or B cell responses, activating the adaptive immune system [15,16]. Finally, HERV-derived promoters or

* Corresponding author. Institute of Virology, School of Medicine, Technical University of Munich, Munich, Germany.
** Corresponding author. Institute of Virology, School of Medicine, Technical University of Munich, Munich, Germany.
E-mail addresses: sabrina.schreiner-gruber@uniklinik-freiburg.de (S. Schreiner), michelle.vincendeau@helmholtz-munich.de (M. Vincendeau).
[1] Contributed equally.

https://doi.org/10.1016/j.micinf.2024.105466
Received 27 March 2024; Received in revised form 8 November 2024; Accepted 16 December 2024
Available online 21 December 2024

enhancers can modulate the expression of inflammatory genes, potentially influencing antiviral immunity [17].

Human Adenoviruses (HAdV) are non-enveloped, double-stranded DNA viruses with 116 types classified into seven species (A-G) (http://hadvwg.gmu.edu). HAdV infections primarily affect the gastrointestinal and respiratory tract, often with mild or self-limiting symptoms [18]. While the global incidence is unclear, infections are common in young children [19] and immunocompromised individuals. HAdV can be lethal in patients with weakened immune systems, particularly in those undergoing allogeneic stem cell transplantation (HSCT) [20], where reactivation of latent virus is associated with increased morbidity and mortality [21,22]. Innate immune responses to HAdV involve interferons (IFNs), which are secreted in response to viral recognition. There are three types of IFNs, each with distinct receptors: IFN-I is found on epithelial cells and responds strongly in the intestine, IFN-III acts on mucosal surfaces [23,24], and IFN-γ (IFN-II) primarily targets immune cells like B lymphocytes and macrophages, with more immunomodulatory than antiviral effects [25]. IFNs can repress HAdV replication in epithelial cells and fibroblasts by targeting the E2F binding site in the E1A enhancer region, inhibiting viral transcription [26]. However, the adenoviral protein E1B–55 K antagonizes IFN-induced genes, illustrating a complex interplay between the virus and host immune responses. In epithelial cells that do not secrete IFNs, the viral proteins may suppress immune defenses, while the presence of IFNs before infection can reduce replication. Type I and II IFNs are mainly produced by lymphocytes in response to pathogens, but HAdV replication is more prominent in epithelial cells [27] than in lymphocytes [24,28]. Persistent HAdV infections [24,29,30] often occur in adenoids and tonsils, with the virus found in T lymphocytes in up to 80 % of pediatric cases. Reactivation in immunosuppressed individuals, particularly those undergoing HSCT, is a major cause of morbidity and mortality. Understanding how cytokine production and interferon pathways regulate HAdV replication is crucial to prevent severe infections and improve patient outcomes in immunocompromised settings.

Here, we investigated the extent to which HAdV-C5 infection can influence the expression of HERVs and thereby regulate key host genes that in turn influence the host immune response. To this end, we infected HepaRG cells with HAdV-C5 and analyzed changes in the expression of HERVs and cellular genes in the RNAseq datasets. Our bioinformatic analysis shows that several HERV elements as well as HERV LTRs are activated or downregulated after HAdV-C5 infection. The regulated HERV elements included MER elements and HERVL18, which are already known to influence immunological processes. We also identified DEHERV-G pairs, which represent differentially expressed genes within 250 kb of a differentially expressed HERV LTR [9]. Functional enrichment analysis revealed that a significant proportion of these DEHERV-G pairs contain genes associated with immune response pathways and viral carcinogenesis. In addition, we identified an FBXO17 transcript encoding an intronic ERVK9-11 sense sequence in HAdV-C5 infection. Interestingly, FBXO17 has already been described as an important factor in the regulation of the interferon response. Thus, our data show that HAdV-C5 infection causes changes in HERV expression as well as in nearby genes, which are associated with influencing immune regulatory pathways.

2. Methods and materials

2.1. Cell culture

HepaRG and HEK-293 (Sigma-Aldrich Inc) cells were grown in DMEM medium supplemented with 10 % FCS or 5 % FCS, 100 U of penicillin and 100 μg of streptomycin per ml at 37 °C in atmosphere with 5 % CO_2. HepaRG cells were propagated in media additionally supplemented with 5 μg/ml of bovine insulin and 0.5 μM of hydrocortisone. All cell lines were consistently tested for mycoplasma contamination.

2.2. Viruses

In this work, H5*pg*4100, containing an 1863 bp deletion (nt 28,602–30465) in the E3 region, was used as the HAdV-C5 virus, kindly provided by Prof. Thomas Dobner (LIV, Hamburg) [31]. Viruses were propagated in H1299 and HEK 293 cells and titrated in HEK 293 cells as previously described [32].

2.3. Illumina RNA sequencing

Total RNA was isolated from whole-cell lysates with TRIzol reagent (*Invitrogen*) as described by the manufacturer. Strand specific, polyA-enriched RNA sequencing was performed as previously reported [33]. RNA integrity number (RIN) was determined with the *Agilent 2100 BioAnalyzer* (*RNA 6000 Nano Kit*, Agilent). For library preparation, 1 μg of RNA was poly(A) selected, fragmented, and reverse transcribed using the *Elute, Prime, Fragment Mix* (Illumina). A-tailing, adaptor ligation, and library enrichment were performed according to the *TruSeq Stranded mRNA Sample Prep Guide* (Illumina). Quality and quantity of RNA libraries were evaluated using the *Agilent 2100 BioAnalyzer* and the *Quant-iT PicoGreen dsDNA Assay Kit* (Life Technologies). RNA libraries were sequenced as 150 bp paired end runs on an *Illumina HiSeq4000* platform at Helmholtz Zentrum München RNAseq Core Facility. Kallisto (version 0.46.1) was used to quantify transcript abundancies from paired-end RNA-seq reads [34]. The index for Kallisto-pseudoalignment was built using the Genome Reference Consortium Human Build 38 patch release 13 (GRCh38. p13), (91). Differential gene expression was analyzed using the R package sleuth (version 0.30.0) [35].

2.4. HERV annotation

Repetitive sequences were identified in the human genome (version hg38) by RepeatMasker [36] and downloaded from the UCSC Table Browser [37]. In this work we only considered LTR (long terminal repeat) transposons of two types - HERV LTRs and Gypsy LTRs – including their internal portions (HERV-int and Gypsy-int) and LTR sequences, as well as solo LTRs (622,700 elements in total). Association between LTRs and internal portions of transposons was established based on the transposon nomenclature by Kojima [38]. Additionally, we also obtained annotations of transposable elements from the HERVd [39] database. Using the Reannotate [40] software, we identified LTRs located in close proximity (up to 40 kb) of HERV and Gypsy elements as HERV-LTR and Gypsy-LTR elements, respectively, while all other LTRs were considered to be solo LTRs. Reannotate was also employed to conduct defragmentation of internal portions and LTR elements rendered noncontiguous as a consequence of insertions and chromosomal rearrangements.

2.5. RNA-seq data processing

Reads in FASTQ files were aligned to the Ensembl human reference genome (genome assembly: GRCh38) using the STAR (Spliced Transcripts Alignment to a Reference) aligner [41]. A maximum of 20 alignments and no more than two mismatches were allowed for each read. After mapping, the BAM files were used with SQUIRE to quantify the expression of HERVs at the locus level. The SQUIRE output was integrated with the previously established HERVs annotation to generate the read counts of the HERV loci.

2.6. Differential expression analysis

Differential expression analysis was performed using DEseq2 [42] with count metrics combining both HERVs and genes. DESeq2 uses the Wald test for hypothesis testing between infected and uninfected cells. p-value was corrected for multiple testing using the Benjamini and Hochberg method. The HERVs and genes with an adjusted p-value less

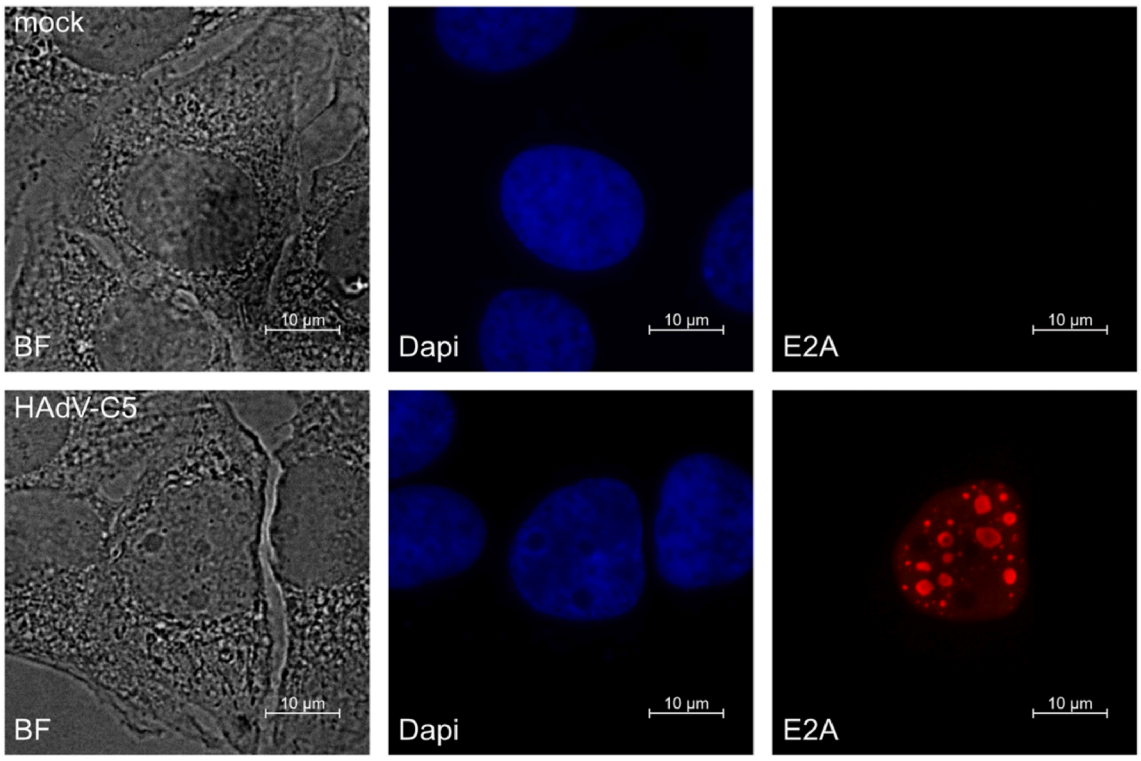

Fig. 1. HAdV-C5 infection of HepaRG cells promotes viral replication centers in the host cell nucleus. HepaRG cells were infected with HAdV-C5 at a multiplicity of infection of 20 FFU/cell. The cells were fixed with 2 % PFA 24 h p. i. and labeled with mAb mouse (α-E2A). Primary Abs were detected with Alexa568 (α-E2A, red) conjugated secondary Abs. Nuclear staining was performed using Dapi. Staining patterns representative of 50 analyzed cells are shown. Scalebar 10 µm. (For interpretation of the references to colour in this figure legend, the reader is referred to the Web version of this article.)

than 0.05 were considered to be significantly differentially expressed.

2.7. Identification of differentially expressed HERV and gene pairs (DEHERV-G pairs)

The count metrics was normalized by DEseq2, using the median of ratios of gene counts relative to the geometric mean per gene for normalization. Correlation analysis was carried out with Differential Gene Correlation Analysis (DGCA), using Pearson correlation coefficient. It identified the differential correlations between HERVs and genes in human adenovirus C serotype 5 (HAdV-C5) infected cells compared to uninfected cells. Following [9], for each differentially expressed HERV locus, we identified the nearest DE gene within 250 kbp on the same strand. The protein-coding genes occurring in the DEHERV-G pairs were subjected to functional enrichment analysis.

2.8. Functional enrichment analysis

Enrichment analysis of GO (Gene Ontology) biological processes and KEGG (Kyoto Encyclopedia of Genes and Genomes) pathways was performed using DAVID (Database for Annotation, Visualisation and Integrated Discovery). The GO biological processes and KEGG pathways were used with a False Discovery Rate (FDR)-adjusted p-value of less than 0.05, meaning that less than 5 % of significant tests lead to false positive results.

2.9. Protein analysis and antibodies (Ab)

Cells were harvested according to the experimental setup and resuspended in RIPA buffer freshly supplemented with 0.2 mM PMSF, 1 mg/ml Pepstatin A, 5 mg/ml aprotinin, 20 mg/ml leupeptin, 25 mM iodacetamide and 25 mM N-ethylmaleimide as previously described [43]. The cell lysates were incubated 30 min on ice, sonicated for 30 s, and the insoluble debris was pelleted at 11,000 rpm/4 °C. Protein concentration was measured and lysates were boiled for 5 min at 95 °C in 2x Laemmli buffer and subsequently analyzed by Western blotting. Primary Abs specific for HAdV proteins used in this study included E2A mouse mAb B6-8 [44]. Primary Ab specific for cellular proteins included monoclonal mouse Ab against β-actin AC-15 (A5441; *Sigma-Aldrich*) and polyclonal rabbit antibody raised against FBXO17 (12,844-1AP; *Proteintech*).

2.10. Indirect immunofluorescence

Cells were cultivated on glass cover slips and infected. Immunofluorescence studies were performed using previously defined protocols [45]. Digital images were acquired using a *Pearson's correlation* coefficient, determined with *ZEISS* software, to analyze colocalization of FBOX17 and viral proteins. Images were cropped in *Adobe Photoshop CS6* and assembled with *Adobe Illustrator CS6*.

2.11. Quantitative real-time PCR analysis

Cells were infected with HAdV-C5 and harvested at 24 h p. i. Total RNA was isolated with TRIzol reagent (Invitrogen) according to the manufacturer's instructions. 1 µg of RNA was reverse transcribed using *Promega* reverse transcription kit, with an anchored oligo (dT)15 primer specific for poly(A) + RNA. Quantitative real-time PCR (qRT-PCR) was performed with a first-strand method with a 1/10 dilution of the cDNA template, 10 pmol/ml of each synthetic oligonucleotide primer, and 5 µl/sample of LunaScript RT SuperMix (*New England BIolabs*). The PCR conditions were as follows: 10 min at 95 °C and 55 cycles of 30 s at 95 °C, 30 s at 55–62 °C, and 30 s at 72 °C. The average threshold cycle (CT) value was determined from biological triplicates, and levels of mRNA were calculated relative to cellular glyceraldehyde-3-phosphate dehydrogenase (GAPDH) mRNA. The identities of reaction products were

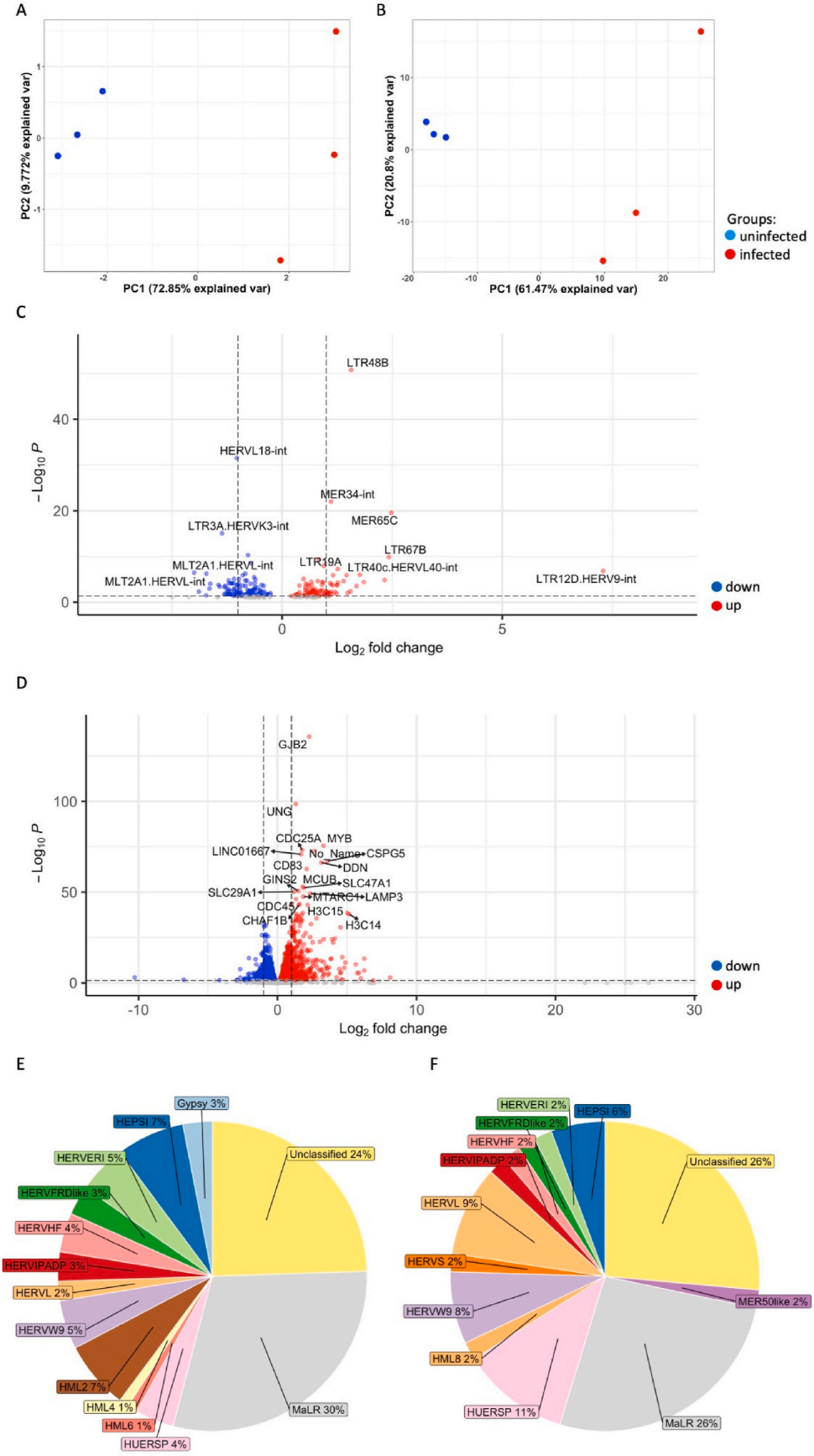

(caption on next page)

Fig. 2. Gene and HERV expression are changed upon HAdV-C5 infection. (A–B) Principal component analysis (PCA) plots of HERVs (A) and genes (B) genes upon HAdV-C5 infection of HepaRG cells. Three technical replicates are shown. (C–D) Volcano plot showing differential HERV expression (C) and gene expression (D) by RNA-seq of infected cells compared to uninfected HepaRG cells. Genes and HERVs in red are significantly differentially upregulated and an adjusted P-value of <0.05. (E–F) Percentage of significantly up (E) or down (F) regulated HERV groups in HAdV-C5 infected cells. (For interpretation of the references to colour in this figure legend, the reader is referred to the Web version of this article.)

Table 1
Differential expression status of DEHERV-G pairs. Symbols ± indicate up/down regulation of genes or HERVs. For example, G+H+ indicates pairs where both a HERV locus and a gene are up-regulated.

Cells	DEHERV-G Pairs			
	G + H+	G + H−	G-H+	G−H−
HAdV-C5 infection	174	24	90	150

validated by melting-curve analysis.

3. Results

3.1. HAdV-C5 infection changes HERV as well as gene expression in HepaRG cells

To explore whether human adenovirus wild-type serotype C5 (HAdV-C5) infection causes changes in HERV expression as well as the expression of host genes, we infected HepaRG cells. Virus infection in these cells was verified by immunofluorescence analyses showing viral replication centers stained by the viral DNA binding protein and infection marker E2A/DBP (Fig. 1).

24 h post-infection, we extracted total RNA, which was subjected to paired-end RNA sequencing. After processing and mapping the raw RNA-seq data the overall similarity between infected and uninfected cells was assessed using principal-component analysis (PCA) of HERVs as well as protein-coding genes. A significant expression shift upon infection was detectable for HERVs (Fig. 2A) and protein-coding genes (Fig. 2B), respectively. Next, we observed the differential expression of HERVs (DEHERVs) and genes (DEGs) between infected and uninfected cells performing differential expression analysis using the DESeq2 R package. 33 HERV loci (Figs. 2C) and 416 genes (Fig. 2D) were significantly up-regulated whereas 48 HERV loci (Figs. 2C) and 184 genes (Fig. 2D) were significantly down-regulated by a fold change of at least 1 in infected cells compared to uninfected. All identified DEHERVs as well as DEGs are listed in Tables S1 and S2. In addition, we performed GO and KEGG enrichment analysis of the protein-coding genes that were upregulated (Figs. S2A and B) or downregulated (Figs. S3A and B) after HAdV-C5 infection. For the identified upregulated genes after HAdV-C5 infection, the analysis revealed that the most enriched BP terms were associated with many biological processes, including several pathways important for RNA processing (Fig. S2A). The same was true for the KEGG analyses (Fig. S2B). For the identified downregulated genes after HAdV-C5 infection, the analysis revealed that the most enriched BP terms (Fig. S3A) and KEGG terms (Fig. S3B) were also associated with many biological processes, including processes related to cellular immune response or cancer development. In addition to the locus-specific DE analysis of HERVs, we used DESeq2 to analyze the general expression trend of the identified HERV elements with non-zero expression levels. Illustrated is the percentage of significantly differentially upregulated (Fig. 2E) as well as downregulated (Fig. 2F) HERV elements after HAdV-C5 infection. DEHERVs from three groups, namely MER50like, HERV-S and HERV-K(HML-8), were upregulated only in HAdV-C5 infected cells, whereas loci belonging to four groups, namely Gypsy, HERV-K(HML-2), HERV-K(HML-4) and HERV-K(HML-6), were downregulated upon adenoviral infection. These findings show that adenoviral infection results in transcriptome changes of HERVs as well as protein-coding genes.

3.2. Pairs of differentially expressed HERVs and genes (DEGERV-G)

Furthermore, we investigated the association between DEGs and the identified upregulated HERV LTRs, which may harbour regulatory elements such as enhancers and promoters [11] and thus may be able to affect genes upstream as well as downstream at a distance of up to 250 kbp [9,16,46]. For each DE-HERV locus, we identified the closest DE gene within 250 kbp on the same strand. Such HERV/gene pairs were termed DEHERV-G pairs. In total, 438 DEHERV-G pairs were identified in cells after HAdV-C5 infection (Table 1). Most DEHERV-G pairs consisted of upregulated genes and HERVs (G + H+), followed by downregulated genes and HERVs (G-H-). In addition, there was a tendency for the number of DEHERV-G pairs to decrease with increasing relative distance between DEGs and DEHERVs under infected conditions (Fig. 3A). Furthermore, we performed GO and KEGG enrichment analysis with the protein-coding genes in close proximity to the up-regulated HERVs (G + H + DEHERV-G pairs) (Table S3). This analysis revealed that several of the most enriched processes were related to the cellular immune response (Fig. 3B). Moreover, one process enriched was viral carcinogenesis also playing an important role for several HAdV oncoproteins encoded in the viral genome (Fig. 3C).

3.3. HAdV-C5 infection results in the upregulation of FBXO17 encoding a sense intronic ERVK9-11 sequence

HERV sequences can create alternative promoters for genes that produce fusion transcripts. Several HERV fusion transcripts have been reported to affect developmental processes [47–49] but also to contribute to disease [48,50]. We therefore took a closer look at our RNA-seq analyses. Interestingly, we found ERVK9-11 and the gene *FBXO17* differentially correlated in HAdV-C5 infected cells compared to control cells (Fig. 4A). FBXO17 has already been reported to negatively regulate IFN-I signaling triggered by double-strand DNA, RNA, or viral infection. To better illustrate the relative expression of both isoforms, we generated a Sashimi plot where each splice junction was plotted and reads were conveniently enumerated. This allowed us to visualize the structure of the *FBXO17* isoforms (Fig. 4B). *FBXO17* shows additional cross-junction reads to the ERVK9-11 loci in HAdV-C5 infected cells (Fig. 4B and Fig. S1), resulting in an FBXO17 transcript encoding a sense intronic ERVK9-11 sequence. It is interesting to note that several intergenic non-coding RNAs have been reported to directly regulate genes in cis and trans [51,52]. However, further functional analysis will be needed to elucidate gene regulation by ERV-encoded long non-coding RNAs.

Moreover, we performed HAdV-C5 virus infections and after indicated time points (24-72hpi) the cells were harvested, lysed, and subjected to immunoblot analysis using an FBXO17 specific antibody. As shown above, E2A was used to control virus infection. FBXO17 protein levels showed several significant differences compared to mock cell lysates without virus infection (Fig. 5A, lanes 1, 3 and 5). Interestingly, we observed several proteins that only appear in the HAdV-C5 lysates (Fig. 5A, lanes 2, 4 and 6; *) indicating different potential isoforms that might appear due to an intronic HERV-sequence. To exclude that the proteins detected were not HAdV capsid proteins, we also stained the samples with an anti-capsid antibody (Fig. 5A). We also analyzed the relative expression of FBXO17 and observed a significant increase upon HAdV-C5 infection in HepaRG cells (Fig. 5B).

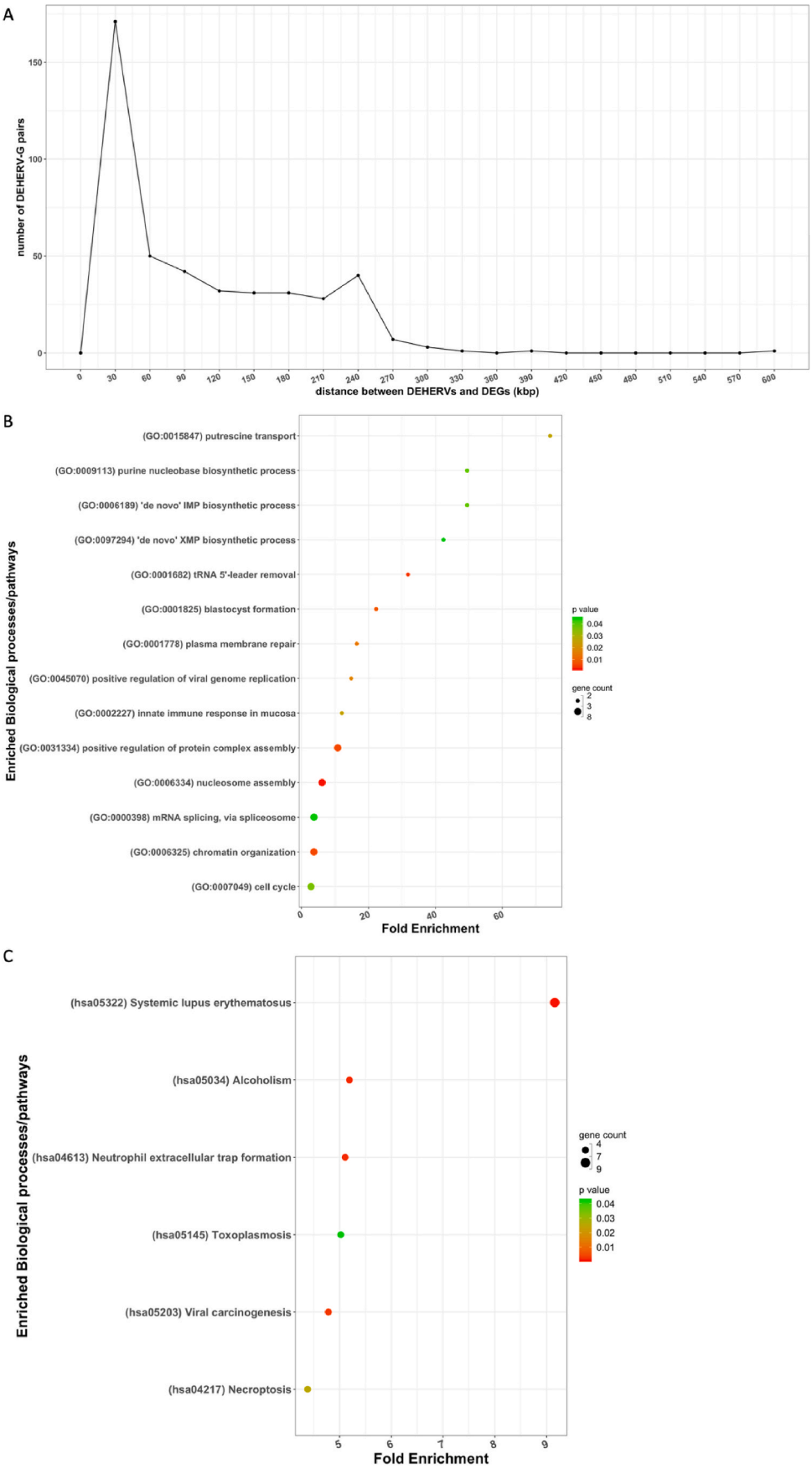

(caption on next page)

Fig. 3. (next page): Distribution and GO analysis of DEHERVG pairs. A) Shown is the distribution of distances between DEGs and DEHERVs within DEHERV-G pairs. Overlapping DEGs and DEHERVs correspond to zero distances (B) Significantly enriched GO terms for biological processes associated with G + H + DEHERV-G pairs. Terms are ordered by fold enrichment. (C) Significantly enriched KEGG pathways associated with G + H + DEHERV-G pairs. Terms are ordered by fold enrichment and their p-value of less than 0.05, with Benjamini-Hochberg-corrected p-values less than 0.05.

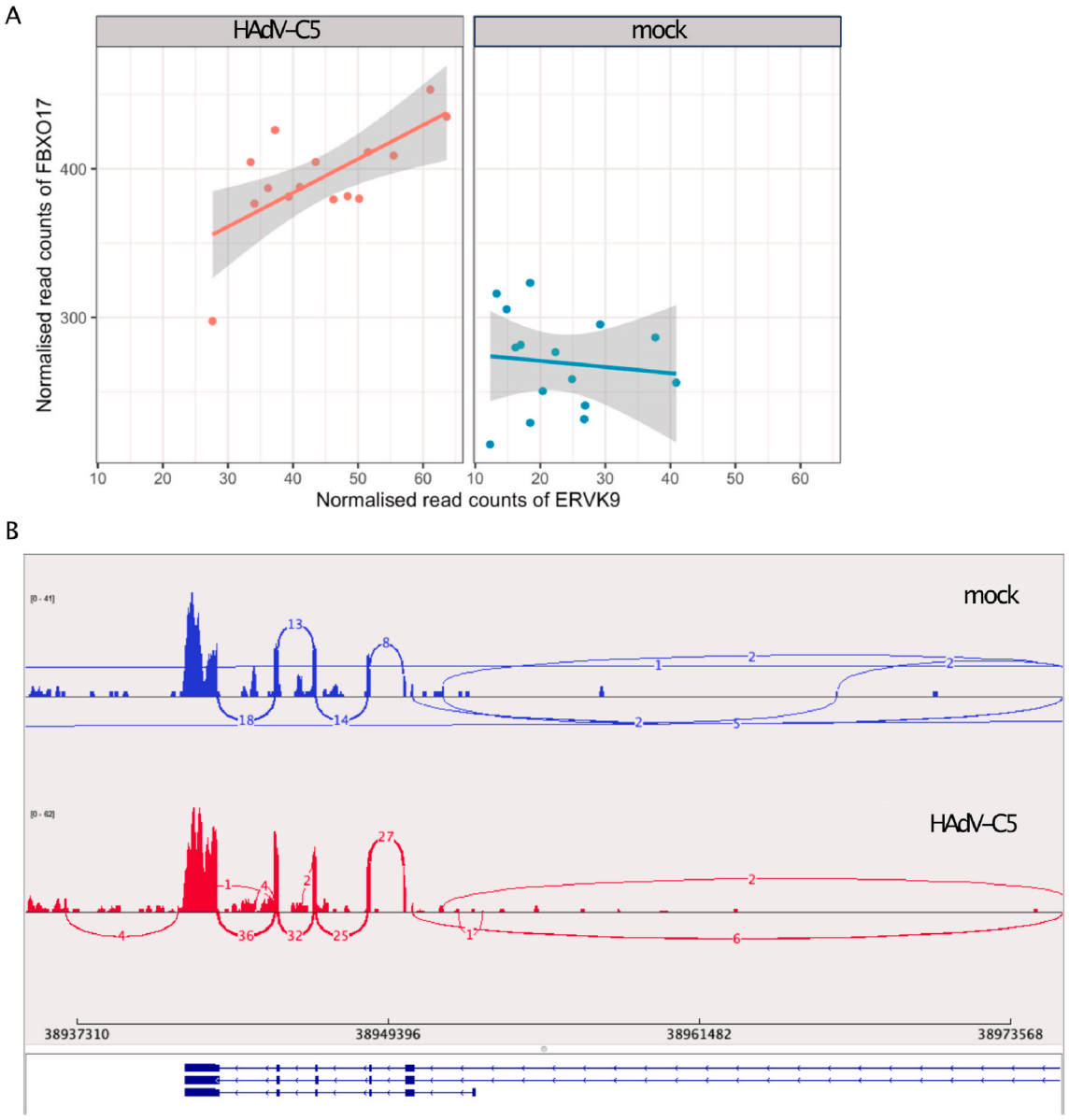

Fig. 4. An FBXO17 encoding a sense intronic ERVK9-11 sequence is made upon HAdV-C5 infection. (A) Scatter plot of HERV locus expression versus gene expression. The ERVK9-11 loci and FBXO17 show differential correlation in HAdV-C5 infected cells compared to uninfected cells according to the DGCA result. (B) A Sashimi plot of *FBXO17* from HAdV-C5 infected and uninfected cells. Raw reads are visualized by bar height and splice junctions, and their respective read numbers are shown by the connecting arcs.

4. Discussion

Hundreds of thousands of HERVs, ranging from full-length proviruses to short gene fragments, influence the antiviral immune response through various mechanisms. For instance, ERV-derived nucleic acids can trigger antiviral recognition, while ERV-derived lncRNAs regulate immune responses. Endogenous retroviral proteins can modulate immunity, and retroviral envelope proteins may block virus entry receptors [12]. Reactivation of specific HERV groups by infections, such as HIV-1, HCV, and IAV [7–9], can impact gene networks [11,46,53,54], particularly via LTRs acting as promoters or enhancers, influencing inflammatory gene expression [12,15,17].

Viruses like HAdV, HCMV, EBV, HIV, and IAV antagonize host immune defenses by blocking INF receptors or disrupting STAT signaling [55]. For example, IFN-mediated repression of HAdV production in epithelial cells and fibroblasts is time-dependent and influenced by IFN levels prior to infection. This suggests that viral proteins may suppress immune defenses in epithelial cells, while IFN presence could reduce HAdV replication [56,57]. These findings are relevant for understanding HAdV reactivation in immunosuppressed patients.

This study aimed to explore how HAdV-C5 infection affects HERV expression and host gene networks. We observed differential activation

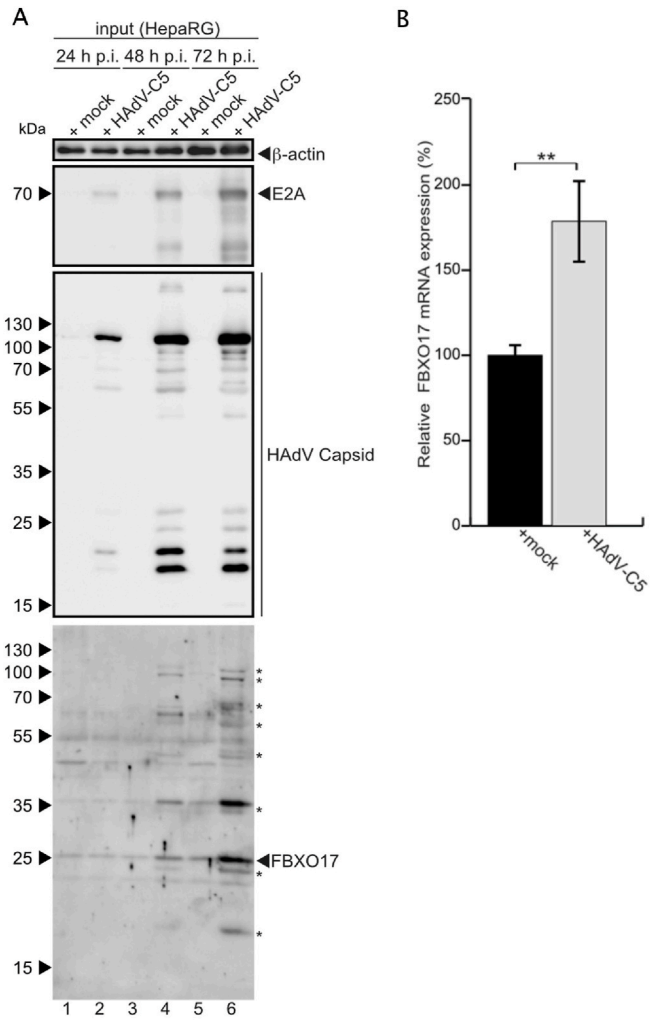

Fig. 5. FBXO17 expression after HAdV infection. HepaRG cells were infected with HAdV-C5. (A) Cells were harvested after 24, 48 and 72 h post infection. Uninfected cells served as mock control. FBXO17 expression was detected using an FBXO17 specific antibody. β-actin was used as a loading control and E2A to proof virus infection. (B) Relative transcript levels of FBXO17 upon HAdV-C5 infection using qRT-PCR, Two-tailed, unpaired T-test, p value 0.00503.

of HERV elements, with LTR48B, MER34-int, MER65C, and LTR67B showing the strongest upregulation, while HERVL18-int, LTR3A, and MLT2A1 were significantly downregulated, some of which are linked to immune regulation.

LTR48 B is the element that shows the strongest activation after HAdV-C5 infection. Not much is known about LTR48B, except that a subset of LTR48B elements has acquired enhancer activity in pluripotent cells [58]. It has also been described that a significant enrichment for the ERV1 groups as a whole, in particular for the members of the LTR48, HERV4, MER41D and HERVFH19 subgroups, occurs after INF–I stimulation [59]. Thus, an indirect effect of activation of LTR48B via INF–I may also be possible. Another upregulated element identified upon HAdV-C5 infection MER-34-int as well as MER65B. Nothing is known about MER34-int in relation to immunological processes. It has been shown that autistic children and their mothers have high expression of MER34 in association with the expression of cytokines such as tumor necrosis factor alpha (TNF-α), interferon gamma (IFN-γ) and IL-10 [60]. Moreover, the MER34 HERV locus transcribes for a unique Env protein called HEMO. HEMO has been detected in the placenta and various cancers and has been shown to be released into the human circulation [61,62]. HEMO has been shown to be regulated by the WNT/b-catenin pathway, to be a “stemness marker” of the normal cell and to be a potential target for immunotherapeutic approaches in tumors [61,62]. Also, MER65B has not yet been implicated in immunological processes. MER65B was previously shown to be dysregulated after SARS-CoV infection [63] and was also detected in tumor tissue and immune cells [64]. MER41 elements were found in the vicinity of immune genes such as AIM2, APOL1, IFI6 and SECTM1, and CRISPR/Cas9-mediated deletion of these elements abolished the responsiveness of the neighboring immune gene IFN-γ [15]. This is an example of how MER elements can be involved in immunological processes and further studies will show whether this is also true for MER34 and MER65 elements. Silencing of SETDB1 in acute myeloid leukaemia cells resulted in the upregulation of numerous HERV groups, including HERVL18. HERV upregulation was bidirectional and was accompanied by the induction of an antiviral response, INF–I signaling and ISG expression. Knockout of either the ssRNA receptor RIG-I or the dsRNA receptor MDA5 abolished this response [65]. In our study we found that HERVL18 was downregulated after HAdV-C5 infection, which would presumably have no effect on interferon signaling. However, further studies would be needed to investigate this in more detail.

Previous studies have shown that many HERV groups have the potential to act as interferon enhancers and promote the development of transcriptional networks associated with the interferon response [12]. Interestingly, several of the DEGs identified in our study, which are in close proximity to the DEHERVs analyzed and were both upregulated following HAdV-C5 infection, were also associated with immune responses. We identified ERVK9-11 and FBXO17 being differentially correlated in HAdV-C5 infected HepaRG cells. Moreover, upon HAdV-C5 infection several unique reads could be mapped against an FBXO17 transcript encoding a sense intronic ERVK9-11 sequence. Interestingly, the F-box protein FBXO17 is known to negatively regulate viral infection-induced IFN-I signaling [66]. FBXO17 specifically interacts with IFN regulatory factor 3 (IRF3) and reduces its dimerisation and nuclear translocation. The decrease in IRF3 dimerisation and nuclear translocation could be attributed to FBXO17-mediated recruitment of protein phosphatase 2 (PP2A), leading to dephosphorylation of IRF3. Thus, an ERVK9-11-FBXO17 transcript, which may arise following HAdV-C5 infection, might play a novel role in the HAdV-mediated INF–I immune response. Interestingly, approximately 20 % of lncRNAs are derived from HERV sequences [67]. Recent studies have emphasized the functional importance of Transpsosable Element-derived sequences in modulating the expression and function of lncRNAs involved in various biological processes such as development and immune response [68–71]. HERV-derived lncRNAs have been shown to regulate the immune response to viral infection by modulating the expression of immune-related genes [69]. The exact mechanisms remain to be fully understood. Future studies investigating additional cell types and HAdV members will provide valuable insights into common HERVs and gene patterns that are reactivated. Moreover, ongoing advancements in sequencing technologies and computational algorithms are expected to further our understanding of the role of HERV-derived lncRNAs in key biological processes.

Overall, our results suggest that individual HERV groups/elements and neighboring genes are upregulated after HAdV-C5 infection and are associated with the regulation of the antiviral immune response. This could indicate that viruses have developed strategies to circumvent HERV-mediated immunity. In the future, functional studies will be necessary to elucidate the exact mechanisms that lead to the activation of HERV immune networks after viral infection.

CRediT authorship contribution statement

Wen Liang: Writing – review & editing, Visualization, Validation, Formal analysis, Data curation. **Miona Stubbe:** Writing – review & editing, Visualization, Validation, Methodology, Investigation, Data curation. **Lisa Pleninger:** Investigation, Data curation. **Anna Hofferek:** Methodology. **Hans Stubbe:** Writing – review & editing, Visualization,

Methodology, Data curation. **Julia Mai:** Methodology. **Salih Özer:** Data curation. **Dmitrij Frishman:** Writing – review & editing, Methodology. **Sabrina Schreiner:** Writing – review & editing, Writing – original draft, Validation, Supervision, Methodology, Investigation, Funding acquisition, Data curation, Conceptualization. **Michelle Vincendeau:** Writing – review & editing, Writing – original draft, Visualization, Validation, Supervision, Funding acquisition, Formal analysis, Data curation, Conceptualization.

Funding

MV was funded by the Deutsche Forschungsgemeinschaft (RTG2668, Project B2, Project-ID:435874434), Sachbeihilfe (496872373), Sachbeihilfe (498956525), Sachbeihilfe (497803923). SS was funded by the Deutsche Forschungsgemeinschaft (DFG, German Research Foundation) under Germany's Excellence Strategy - EXC 2155 - project number 390874280 and by the Deutsche Forschungsgemeinschaft (DFG, German Research Foundation) – Projektnummer 272983813 – TRR179. This project was also partially funded by the Deutsche Forschungsgemeinschaft (DFG, German Research Foundation) in the framework of the Research Unit FOR5200 DEEP-DV (443644894) project 08.

Declaration of competing interest

We declare no competing interests.

Acknowledgments

We thank Ulrike Protzer and Ruth Brack-Werner for scientific discussions.

Appendix B. Supplementary data

Supplementary data to this article can be found online at https://doi.org/10.1016/j.micinf.2024.105466.

References

[1] Jakobsson J, Vincendeau M. SnapShot: human endogenous retroviruses. Cell 2022;185(2):400–400.e1.
[2] Mager DL, Medstrand P. Retroviral repeat sequences. In: Cooper D, editor. Nature encyclopedia of the human genome. London: Nature Publishing Group; 2003. p. 2003.
[3] Makałowski W. The human genome structure and organization. Acta Biochim Pol 2001;48(3):587–98.
[4] Lander ES, et al. Initial sequencing and analysis of the human genome. Nature 2001;409(6822):860–921.
[5] Osmanski AB, et al. Insights into mammalian TE diversity through the curation of 248 genome assemblies. Science 2023;380(6643):eabn1430.
[6] Buzdin A, et al. At least 50% of human-specific HERV-K (HML-2) long terminal repeats serve in vivo as active promoters for host nonrepetitive DNA transcription. J Virol 2006;80(21):10752–62.
[7] Vincendeau M, et al. Modulation of human endogenous retrovirus (HERV) transcription during persistent and de novo HIV-1 infection. Retrovirology 2015;12:27.
[8] Weber M, et al. Increased HERV-K(HML-2) transcript levels correlate with clinical parameters of liver damage in hepatitis C patients. Cells 2021;10(4).
[9] Liu H, et al. Influenza A virus infection reactivates human endogenous retroviruses associated with modulation of antiviral immunity. Viruses 2022;14(7).
[10] Wells JN, Feschotte C. A field Guide to eukaryotic transposable elements. Annu Rev Genet 2020;54:539–61.
[11] Feschotte C. Transposable elements and the evolution of regulatory networks. Nat Rev Genet 2008;9(5):397–405.
[12] Srinivasachar Badarinarayan S, Sauter D. Switching sides: how endogenous retroviruses protect us from viral infections. J Virol 2021;95(12).
[13] Wang X, et al. Human endogenous retrovirus W family envelope protein (HERV-W env) facilitates the production of TNF-α and IL-10 by inhibiting MyD88s in glial cells. Arch Virol 2021;166(4):1035–45.
[14] Zhou B, et al. Endogenous retrovirus-derived long noncoding RNA enhances innate immune responses via derepressing RELA expression. mBio 2019;10(4).
[15] Chuong EB, Elde NC, Feschotte C. Regulatory evolution of innate immunity through co-option of endogenous retroviruses. Science 2016;351(6277):1083–7.
[16] Wang M, et al. Transcription profile of human endogenous retroviruses in response to dengue virus serotype 2 infection. Virology 2020;544:21–30.
[17] Srinivasachar Badarinarayan S, et al. HIV-1 infection activates endogenous retroviral promoters regulating antiviral gene expression. Nucleic Acids Res 2020;48(19):10890–908.
[18] Khanal S, Ghimire P, Dhamoon AS. Reply to the Comment on: Subrat Khanal et al. The Repertoire of Adenovirus in Human Disease: The Innocuous to the Deadly. Biomedicines 2018;6:30. Biomedicines, 2019. 7(1).
[19] Cooper RJ, et al. The epidemiology of adenovirus infections in Greater Manchester, UK 1982-96. Epidemiol Infect 2000;125(2):333–45.
[20] Dailey Garnes NJM, Ragoonanan D, Aboulhosn A. Adenovirus infection and disease in recipients of hematopoietic cell transplantation. Curr Opin Infect Dis 2019;32(6):591–600.
[21] Hiwarkar P, et al. Impact of viral reactivations in the era of pre-emptive antiviral drug therapy following allogeneic haematopoietic SCT in paediatric recipients. Bone Marrow Transplant 2013;48(6):803–8.
[22] Kosulin K, et al. Persistence and reactivation of human adenoviruses in the gastrointestinal tract. Clin Microbiol Infect 2016;22(4):381.e1–8.
[23] Mahlakõiv T, et al. Leukocyte-derived IFN-α/β and epithelial IFN-λ constitute a compartmentalized mucosal defense system that restricts enteric virus infections. PLoS Pathog 2015;11(4):e1004782.
[24] Pulverer JE, et al. Temporal and spatial resolution of type I and III interferon responses in vivo. J Virol 2010;84(17):8626–38.
[25] Valente G, et al. Distribution of interferon-gamma receptor in human tissues. Eur J Immunol 1992;22(9):2403–12.
[26] Sherwood V, et al. Improved growth of enteric adenovirus type 40 in a modified cell line that can no longer respond to interferon stimulation. J Gen Virol 2007;88(Pt 1):71–6.
[27] Garnett CT, et al. Latent species C adenoviruses in human tonsil tissues. J Virol 2009;83(6):2417–28.
[28] Azzi JR, Sayegh MH, Mallat SG. Calcineurin inhibitors: 40 years later, can't live without. J Immunol 2013;191(12):5785–91.
[29] Kosulin K, et al. Intestinal adenovirus shedding before allogeneic stem cell transplantation is a risk factor for invasive infection post-transplant. EBioMedicine 2018;28:114–9.
[30] Zheng Y, Stamminger T, Hearing P. E2F/Rb family proteins mediate interferon induced repression of adenovirus immediate early transcription to promote persistent viral infection. PLoS Pathog 2016;12(1):e1005415.
[31] Schreiner S, et al. Proteasome-dependent degradation of Daxx by the viral E1B-55K protein in human adenovirus-infected cells. J Virol 2010;84(14):7029–38.
[32] Catalucci D, et al. An adenovirus type 5 (Ad5) amplicon-based packaging cell line for production of high-capacity helper-independent deltaE1-E2-E3-E4 Ad5 vectors. J Virol 2005;79(10):6400–9.
[33] Haack TB, et al. ELAC2 mutations cause a mitochondrial RNA processing defect associated with hypertrophic cardiomyopathy. Am J Hum Genet 2013;93(2):211–23.
[34] Bray NL, et al. Near-optimal probabilistic RNA-seq quantification. Nat Biotechnol 2016;34(5):525–7.
[35] Pimentel H, et al. Differential analysis of RNA-seq incorporating quantification uncertainty. Nat Methods 2017;14(7):687–90.
[36] Smit A, Hubley R, Green P. RepeatMasker open. 2013. 2015.
[37] Karolchik D, et al. The UCSC Table Browser data retrieval tool. Nucleic Acids Res 2004;32(Database issue):D493–6.
[38] Kojima KK. Human transposable elements in Repbase: genomic footprints from fish to humans, vol. 9. Mob DNA; 2018. p. 2.
[39] Paces J, et al. HERVd: the human endogenous RetroViruses database: update. Nucleic Acids Res 2004;32(Database issue):D50.
[40] Pereira V. Automated paleontology of repetitive DNA with REANNOTATE. BMC Genom 2008;9:614.
[41] Dobin A, et al. STAR: ultrafast universal RNA-seq aligner. Bioinformatics 2013;29(1):15–21.
[42] Love MI, Huber W, Anders S. Moderated estimation of fold change and dispersion for RNA-seq data with DESeq2. Genome Biol 2014;15(12):550.
[43] Stubbe M, et al. Viral DNA binding protein SUMOylation promotes PML nuclear body localization next to viral replication centers. mBio 2020;11(2).
[44] Berscheminski J, et al. Sp100 isoform-specific regulation of human adenovirus 5 gene expression. J Virol 2014;88(11):6076–92.
[45] Kindsmüller K, et al. Intranuclear targeting and nuclear export of the adenovirus E1B-55K protein are regulated by SUMO1 conjugation. Proc Natl Acad Sci U S A 2007;104(16):6684–9.
[46] Fuentes DR, Swigut T, Wysocka J. Systematic perturbation of retroviral LTRs reveals widespread long-range effects on human gene regulation. Elife 2018;7.
[47] Xia B, et al. On the genetic basis of tail-loss evolution in humans and apes. Nature 2024;626(8001):1042–8.
[48] Young JM, et al. DUX4 binding to retroelements creates promoters that are active in FSHD muscle and testis. PLoS Genet 2013;9(11):e1003947.
[49] Mitsuhashi S, et al. Nanopore direct RNA sequencing detects DUX4-activated repeats and isoforms in human muscle cells. Hum Mol Genet 2021;30(7):552–63.
[50] Schulte AM, et al. Human trophoblast and choriocarcinoma expression of the growth factor pleiotrophin attributable to germ-line insertion of an endogenous retrovirus. Proc Natl Acad Sci U S A 1996;93(25):14759–64.
[51] Cao H, et al. Very long intergenic non-coding (vlinc) RNAs directly regulate multiple genes in cis and trans. BMC Biol 2021;19(1):108.
[52] Louro R, Smirnova AS, Verjovski-Almeida S. Long intronic noncoding RNA transcription: expression noise or expression choice? Genomics 2009;93(4):291–8.

[53] Faulkner GJ, et al. The regulated retrotransposon transcriptome of mammalian cells. Nat Genet 2009;41(5):563–71.
[54] Padmanabhan Nair V, et al. Activation of HERV-K(HML-2) disrupts cortical patterning and neuronal differentiation by increasing NTRK3. Cell Stem Cell 2021; 28:1566–1581.e8.
[55] Nan Y, Wu C, Zhang YJ. Interplay between janus kinase/signal transducer and activator of transcription signaling activated by type I interferons and viral antagonism. Front Immunol 2017;8:1758.
[56] Roy S, et al. Adenoviruses in lymphocytes of the human gastro-intestinal tract. PLoS One 2011;6(9):e24859.
[57] Segerman A, et al. Adenovirus types 11p and 35 attach to and infect primary lymphocytes and monocytes, but hexon expression in T-cells requires prior activation. Virology 2006;349(1):96–111.
[58] Casanova M, et al. A primate-specific retroviral enhancer wires the XACT lncRNA into the core pluripotency network in humans. Nat Commun 2019;10(1):5652.
[59] Attig J, et al. Physiological and pathological transcriptional activation of endogenous retroelements assessed by RNA-sequencing of B lymphocytes. Front Microbiol 2017;8:2489.
[60] Cipriani C, et al. Modulation of human endogenous retroviruses and cytokines expression in peripheral blood mononuclear cells from autistic children and their parents. Retrovirology 2022;19(1):26.
[61] Kasperek A, et al. Therapeutic potential of the human endogenous retroviral envelope protein HEMO: a pan-cancer analysis. Mol Oncol 2022;16(7):1451–73.
[62] Heidmann O, et al. HEMO, an ancestral endogenous retroviral envelope protein shed in the blood of pregnant women and expressed in pluripotent stem cells and tumors. Proc Natl Acad Sci U S A 2017;114(32):E6642–e6651.
[63] Gao L, et al. SARS-CoV-2 impacts the transcriptome and epigenome at the maternal-fetal interface in pregnancy. bioRxiv 2022:2022. 05.31.494153.
[64] Wang J, et al. Single-cell RNA sequencing highlights the functional role of human endogenous retroviruses in gallbladder cancer. EBioMedicine 2022;85:104319.
[65] Cuellar TL, et al. Silencing of retrotransposons by SETDB1 inhibits the interferon response in acute myeloid leukemia. J Cell Biol 2017;216(11):3535–49.
[66] Peng D, et al. A novel function of F-box protein FBXO17 in negative regulation of type I IFN signaling by recruiting PP2A for IFN regulatory factor 3 deactivation. J Immunol 2017;198(2):808–19.
[67] Kelley D, Rinn J. Transposable elements reveal a stem cell-specific class of long noncoding RNAs. Genome Biol 2012;13(11):R107.
[68] Kapusta A, et al. Transposable elements are major contributors to the origin, diversification, and regulation of vertebrate long noncoding RNAs. PLoS Genet 2013;9(4):e1003470.
[69] Peng X, et al. Unique signatures of long noncoding RNA expression in response to virus infection and altered innate immune signaling. mBio 2010;1(5).
[70] Chu C, et al. Genomic maps of long noncoding RNA occupancy reveal principles of RNA-chromatin interactions. Mol Cell 2011;44(4):667–78.
[71] Rosa A, et al. The interplay between the master transcription factor PU.1 and miR-424 regulates human monocyte/macrophage differentiation. Proc Natl Acad Sci U S A 2007;104(50):19849–54.